

An ionization region model of the reactive Ar/O₂ high power impulse magnetron sputtering discharge

Jón Tómas Guðmundsson^{1,2}

¹ Department of Space and Plasma Physics,

KTH Royal Institute of Technology, Stockholm, Sweden

² Science Institute, University of Iceland, Reykjavik, Iceland

Department of Physical Electronics, Masaryk University,

Brno, Czech Republic

June 13., 2019

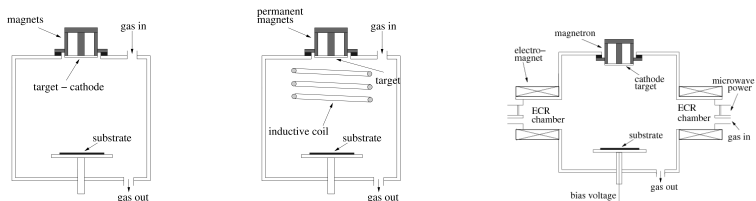


Introduction

- Magnetron sputtering discharges are widely used in thin film processing
- Applications include
 - thin films in integrated circuits
 - magnetic material
 - hard, protective, and wear resistant coatings
 - optical coatings
 - decorative coatings
 - low friction films



Introduction



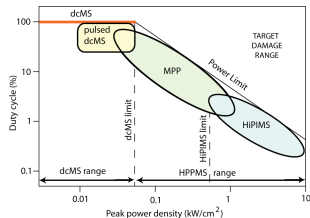
From Gudmundsson (2008), J. Phys.: Conf. Ser. **100** 082002

- A typical dc planar magnetron discharge operates at a pressure of 1 – 10 mTorr with a magnetic field strength of 10 – 50 mT and at cathode potentials 300 – 700 V
- Electron density in the substrate vicinity is in the range $10^{15} - 10^{16} \text{ m}^{-3}$
 - low fraction of the sputtered material is ionized ($\sim 1\%$)
 - the majority of ions are the ions of the inert gas
 - additional ionization by a secondary discharge (rf or microwave)



Introduction

- High ionization of sputtered material requires very high density plasma
- In a conventional dc magnetron sputtering discharge the power density (plasma density) is limited by the thermal load on the target
- High power pulsed magnetron sputtering (HPPMS)
- In a HiPIMS discharge a high power pulse is supplied for a short period
 - low frequency
 - low duty cycle
 - low average power



Gudmundsson et al. (2012), JVSTA **30** 030801

- Power density limits
 $\rho_t = 0.05 \text{ kW/cm}^2$ dcMS limit
 $\rho_t = 0.5 \text{ kW/cm}^2$ HiPIMS limit



Introduction

- Reactive sputtering, where metal targets are sputtered in a reactive gas atmosphere to deposit compound materials is of utmost importance in various technologies
- In reactive sputtering processes a reactive gas O₂, N₂, or CH₄ etc. is mixed to the noble working gas for oxide, nitride, or carbide deposition
- HiPIMS deposition generally gives denser, smoother films and higher crystallinity than dcMS grown films



Helmersson et al. (2006) Thin Solid Films **513** 1

Magnus et al. (2012) IEEE EDL **33** 1045

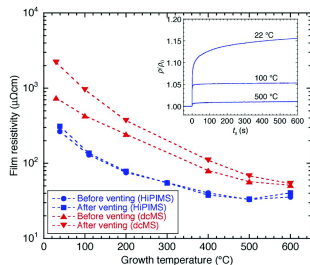


Reactive HiPIMS - Applications



Application – Film Resistivity

- TiN as diffusion barriers for copper and aluminum interconnects
- HiPIMS deposited films have significantly lower resistivity than dcMS deposited films on SiO₂ at all growth temperatures due to reduced grain boundary scattering
- Thus, ultrathin continuous TiN films with superior electrical characteristics and high resistance towards oxidation can be obtained with HiPIMS at reduced temperatures



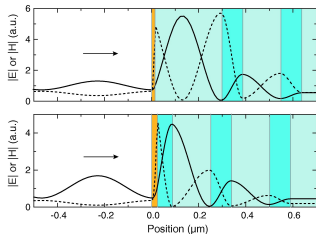
From Magnus et al. (2012) IEEE EDL **33** 1045



Application – Bragg mirror

- Multilayer structures containing a high-contrast (TiO₂/SiO₂) Bragg mirror
- fabricated on fused-silica substrates
 - reactive HiPIMS TiO₂ (88 nm)
 - reactive dcMS SiO₂ (163 nm)
 - capped with semitransparent gold
- Rutile TiO₂ ($n = 2.59$) and SiO₂ ($n = 1.45$) provide a large index contrast
- Smooth rutile TiO₂ films can be obtained by HiPIMS at relatively low growth temperatures, without post-annealing

Agnarsson et al. (2013) TSF 545 445



From Leosson et al. (2012) Opt. Lett. **37** 4026

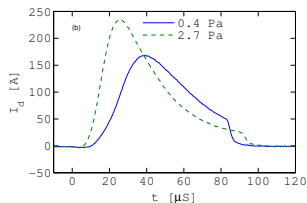
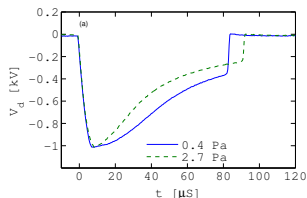
Voltage - Current - Time characteristics

Non-reactive HiPIMS



HiPIMS - Voltage - Current - time

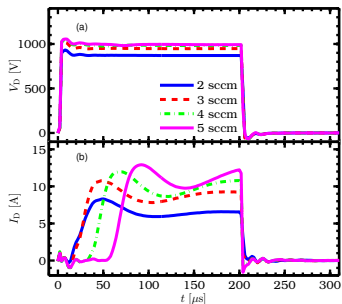
- To describe the discharge current-voltage characteristics the current-voltage-time space is required
- The early work on HiPIMS used 50 – 100 μs pulses and a pulse repetition frequency in the range 50–1000 Hz
- The applied target voltage V_d and target current I_d for an argon discharge at 0.4 and 2.7 Pa. The target is made of copper 150 mm in diameter



From Gudmundsson et al. (2012), JVSTA 30 03080

HiPIMS - Voltage - Current - time

- Modern pulser units have large storage capacitor, the voltage pulse V_D on the cathode can be almost square even for high currents I_D during the full pulse length
- A square voltage pulse is achieved as seen in the discharge voltage and current waveforms for Ar/N₂ discharges operated at different nitrogen flow rates while the argon flow rate was kept fixed at 40 sccm to achieve 0.9 Pa and 150 W average power for 200 μ s pulses



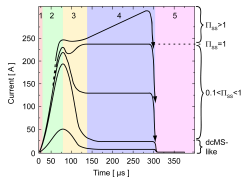
From Hajihoseini and Gudmundsson

(2017), JPD **50** 505302

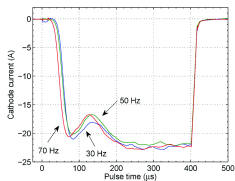


HiPIMS - Voltage - Current - time

- In **non-reactive** discharge the current waveform shows an initial pressure dependent peak that is followed by a second phase that is power and material dependent
- The initial phase has a contribution from the working gas ions, whereas the later phase has a strong contribution from self-sputtering at high voltage



From Gudmundsson et al. (2012), JVSTA 30 030801



From Magnus et al. (2011) JAP 110 083306

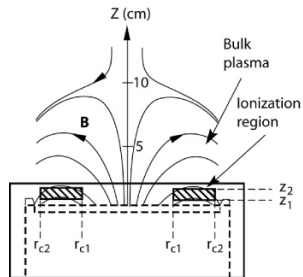


Ionization region model studies of non-reactive HiPIMS



Ionization region model non-reactive HiPIMS

- The ionization region model (IRM) was developed to improve the understanding of the plasma behaviour during a HiPIMS pulse and the afterglow
- The main feature of the model is that an ionization region (IR) is defined next to the race track
- The IR is defined as an annular cylinder with outer radii r_{c2} , inner radii r_{c1} and length $L = z_2 - z_1$, extends from z_1 to z_2 axially away from the target



The definition of the volume covered by the IRM

From Raadu et al. (2011), PSST **20** 065007

Ionization region model non-reactive HiPIMS

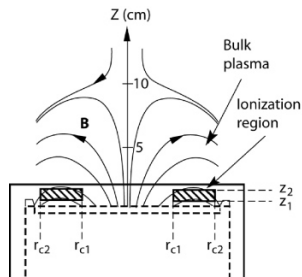
- The temporal development is defined by a set of ordinary differential equations giving the first time derivatives of
 - the electron energy
 - the particle densities for all the particles
- The species assumed in the non-reactive-IRM are
 - cold electrons e^C , hot electrons e^H
 - argon atoms $Ar(3s^23p^6)$, warm argon atoms in the ground state Ar^W , hot argon atoms in the ground state Ar^H , Ar^m ($1s_5$ and $1s_3$) (11.6 eV), argon ions Ar^+ (15.76 eV)
 - titanium atoms $Ti(a^3F)$, titanium ions Ti^+ (6.83 eV), doubly ionized titanium ions Ti^{2+} (13.58 eV)
 - aluminium atoms $Al(2P_{1/2})$, aluminium ions Al^+ (5.99 eV), doubly ionized aluminium ions Al^{2+} (18.8 eV)

Detailed model description is given in Huo et al. (2017), JPD 50 354003



Ionization region model non-reactive HiPIMS

- Geometrical effects are included indirectly as loss and gain rates across the boundaries of this annular cylinder to the target and the bulk plasma
- The electron density is found assuming quasi-neutrality of the plasma



The definition of the volume covered by the IRM

From Raadu et al. (2011), PSST **20** 065007



Ionization region model non-reactive HiPIMS

- The particle balance equation for a particular species is given by

$$\frac{dn_{\text{species}}}{dt} = \sum R_{\text{species,process}}$$

- The reaction rate $R_{j,\text{volume}}$ for a given volume reaction of a species j is

$$R_{j,\text{volume}} = k \times \prod_i n_{r,i} \quad [\text{m}^{-3}\text{s}^{-1}]$$

- The rate at which species are sputtered off the target (Al, Ti and O) is

$$R_{n,\text{sputt}} = \frac{\sum_i \Gamma_i^{\text{RT}} S_{\text{RT}} Y_i(E)}{V_{\text{IR}}}$$

and i stands for the ion involved in the process, here $i = \text{Al}^+, \text{Al}^{2+}, \text{Ti}^+, \text{Ti}^{2+}, \text{Ar}^+, \text{O}^+, \text{and } \text{O}_2^+$, Γ_i^{RT} is the flux of ion i towards the target



Ionization region model non-reactive HiPIMS

- For each ion there is a loss rate given as

$$R_{i,\text{loss}} = - \frac{\Gamma_i^{\text{BP}} S_{\text{BP}} + \Gamma_i^{\text{RT}} S_{\text{RT}}}{V_{\text{IR}}}$$

where i stands for the particular ion and S_{BP} is the area of the annular cylinder facing the lower density plasma outside the IR (bulk plasma), and Γ_i^{BP} is the flux of ion i across the boundary towards the lower density plasma

- Thus the flux out of the IR towards the lower density plasma is reduced as required to obtain the assumed ion back-attraction probability β

$$\Gamma_i^{\text{BP}} = \left(\frac{1}{\beta} - 1 \right) \frac{S_{\text{IR}}}{S_{\text{BP}}} \Gamma_i^{\text{RT}}$$



Ionization region model non-reactive HiPIMS

- Gas rarefaction lowers the density of the working gas inside the IR below the value in the surrounding gas reservoir, $n_{g,0}$
- This gives a back-diffusion (gain) term

$$R_{g,\text{refill}} = \frac{1}{2} v_{\text{ran}} \frac{(n_{g,0} - n_g) S_{\text{RT}}}{V_{\text{IR}}}$$

where the subscript g stands for the atoms and molecules of the working gas Ar and O₂



Ionization region model non-reactive HiPIMS

- The return flux of recombined positive argon ions Ar⁺ from the target is treated as two groups of atoms with different temperatures
 - a hot component Ar^H that returns from the target with a typical sputter energy of a few electron volts
 - a warm component Ar^W that is assumed to be embedded in the target at the ion impact, and then return to the surface and finally leave with the target temperature, at most 0.1 eV
- Thus there is a loss out of the IR

$$R_{\text{Ar}^Z, \text{loss}} = -v_{\text{ran}} n_{\text{Ar}^Z} \frac{S_{\text{RT}}}{V_{\text{IR}}}$$

where Z stands for H for hot or W for warm argon atoms



Ionization region model non-reactive HiPIMS

- In addition there is a change in the neutral density due to kick-out by collisions with fast sputtered atoms coming from the target
- For each of the neutrals Y of the working gas, including each of the metastable states, the particle balance includes a loss term

$$R_{n,\text{kick-out}} = -\frac{1}{2} \frac{v_{\text{ran},X}}{L} F_{\text{coll}} \frac{M_X}{M_Y} \frac{\sum_i n_{X,i}}{\sum_i n_{Y,i}} n_Y$$

- The sum is taken over all the states of that sputtered species and

$$F_{\text{coll}} = 1 - \exp(-L/\lambda_{X,\text{gas}})$$

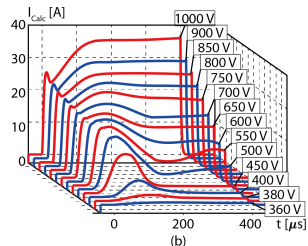
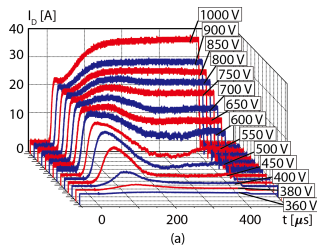
is the probability of a collision inside the IR, where $\lambda_{X,\text{gas}}$ is the mean free path for an atom X sputtered off the target

Ionization region model non-reactive HiPIMS

- The IRM is a semi-empirical model in the sense that it uses a measured discharge current waveform as a main input parameter
- Measured and calculated temporal variations of the discharge current for various discharge (cathode) voltages for a 50 mm diameter Al target

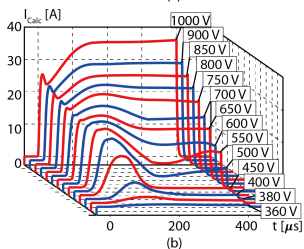
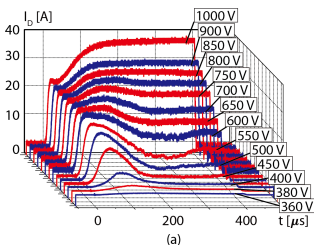
From Huo et al. (2017) JPD **50** 354003

Experimental data from Anders et al. (2007) JAP **102** 113303



Ionization region model non-reactive HiPIMS

- The model needs to be adapted to an existing discharge (the geometry and pressure, the process gas, sputter yields, target species, and a reaction set for these species) and then fitted to two or three parameters
 - The voltage drop across the IR, V_{IR} , accounts for the power transfer to the electrons
 - The probability of back-attraction of ions to the target β
 - The probability r of back-attraction of secondary electrons emitted



From Huo et al. (2017) JPD **50** 354003

Experimental data from Anders et al. (2007) JAP **102** 113303

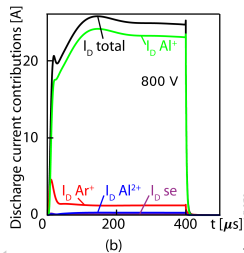
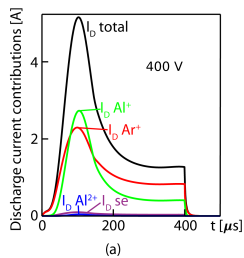


Ionization region model non-reactive HiPIMS

- A **non-reactive** discharge with Al target
- When the discharge is operated at 400 V the contributions of Al⁺ and Ar⁺-ions to the discharge current are very similar
- At 800 V Al⁺-ions dominate the discharge current (**self-sputtering**) while the contribution of Ar⁺ is below 10 % except at the initiation of the pulse

From Huo et al. (2017), JPD **50** 354003

Experimental data from Anders et al. (2007) JAP **102** 113303

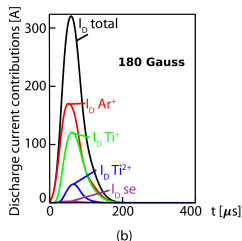
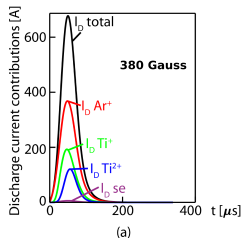


Ionization region model non-reactive HiPIMS

- A **non-reactive** discharge with Ti target
- The contributions to the discharge current for two cases, weak (180 Gauss) and strong (380 Gauss) magnetic field, at 75 Hz pulse frequency
- Stronger magnetic field leads to a higher discharge current
- Higher magnetic field strength leads to higher relative contribution of Ti²⁺ while it lowers the relative contribution of Ti⁺

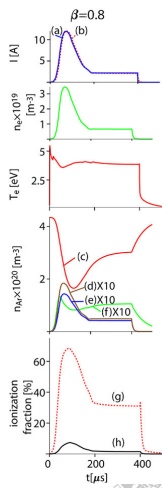
From Huo et al. (2017), JPD **50** 354003

Experimental data from Bradley et al. (2015) JPD **48** 215202



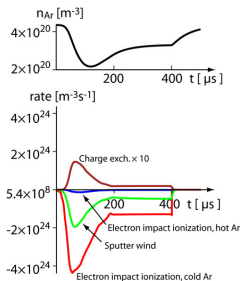
Ionization region model non-reactive HiPIMS

- The discharge current (a) experimentally recorded and (b) calculated
- Electron density and electron temperature
 - (c) argon working gas density
 - (d) argon ion density n_{Ar^+} ,
 - (e) hot recombined argon density n_{Ar^H}
 - (f) metastable argon density n_{Ar^m}
 - (g) ionized density fraction of the sputtered species (aluminum), $F_{density,Al}$
 - (h) ionized density fraction of the argon working gas, $F_{density,Ar}$
- The discharge was operated in argon at 1.8 Pa with a 2 inch Al target, with a pulse voltage of 450 V and a peak discharge current of 12 A



Ionization region model non-reactive HiPIMS

- One important process is gas rarefaction, which results in a depletion of the working gas density in the near-cathode region
- The rate of gas rarefaction dn_{Ar}/dt is the fastest at the maximum in discharge current, and a highest absolute value of the gas rarefaction $\Delta n_{\text{Ar}}/n_{\text{Ar},0} \approx 50\%$ (top black curve) appears 40 – 60 μs after the discharge current maximum
- After the pulse is turned off ($t = 400 \mu\text{s}$) the gas refills and, with a time constant of 100 – 120 μs , returns to the initial value $n_{\text{Ar},0}$

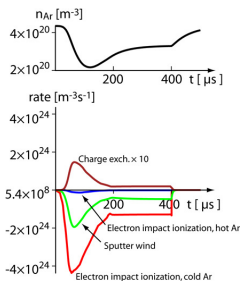


From Huo et al. (2012), PSST 21 045004



Ionization region model non-reactive HiPIMS

- The processes that make contribution to gas rarefaction in a HiPIMS discharge with argon as working gas at 1.8 Pa, Al target and $V_D = 450$ V
- The dominating loss terms are
 - electron impact ionization
 - sputter wind kick-out
- The ionization term is larger by more than a factor of two throughout the pulse
- Most of the sputter wind would therefore pass through the dense ionization region without colliding with a working gas atom

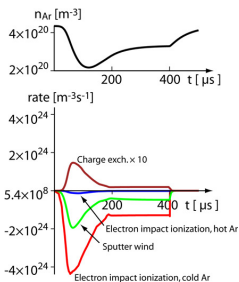


From Huo et al. (2012), PSST 21 045004



Ionization region model non-reactive HiPIMS

- The fraction of Ar⁺ ions that are not attracted to the target ($1 - \beta_g$) leaves to the bulk plasma and is lost
- The remaining fraction β_g impinges on the target, picks up an electron, and returns as a part of a hot population n_{Ar^H}
- The Ar^H returns with an equivalent temperature of 2 eV, giving an average speed of about 3 km/s and does not collide inside the ionization region and pass through it in about 2 – 4 μ s
- The result is that argon atoms can be regarded as in practice lost upon ionization



From Huo et al. (2012), PSST 21 045004



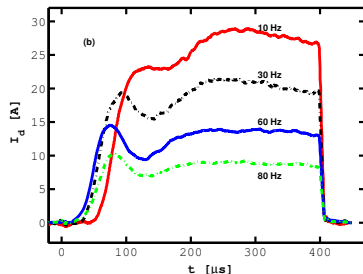
Voltage - Current - Time characteristics

Reactive HiPIMS



HiPIMS - Voltage - Current - time

- During **reactive sputtering**, a reactive gas is added to the inert working gas
- The current waveform in the reactive Ar/N₂ HiPIMS discharge with Ti target is highly dependent on the pulse repetition frequency
- N₂ addition changes the plasma composition and the target condition can also change due to the formation of a compound on its surface

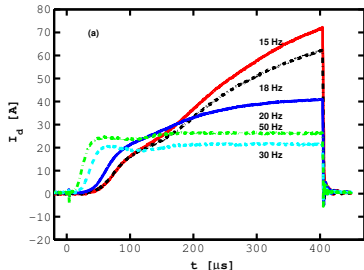


After Magnus et al. (2011) JAP **110** 083306



HiPIMS - Voltage - Current - time

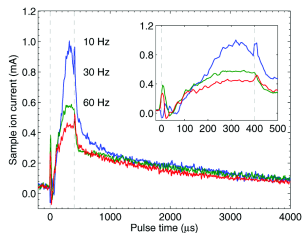
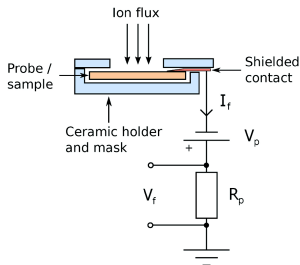
- Similarly for the Ar/O₂ discharge, the current waveform is highly dependent on the repetition frequency and applied voltage which is linked to oxide formation on the target
- The current is found to increase significantly as the frequency is lowered



After Magnus et al. (2012), JVSTA **30** 050601

HiPIMS - Voltage - Current - time

- The observed changes in the discharge current are reflected in the flux of ions impinging on the substrate



From Magnus et al. (2011), JAP **110** 083306

HiPIMS - Voltage - Current - time

- The discharge current I_D is the sum of the ion current I_i and the secondary electron current $I_i\gamma_{SE}$ or

$$I_D = I_i(1 + \gamma_{SE})$$

where γ_{SE} is the secondary electron emission coefficient of the target material

- Also

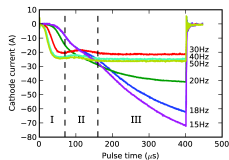
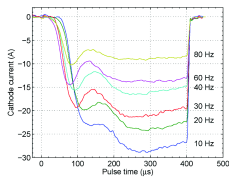
$$I_i \propto n_i \propto \frac{1}{\mathcal{E}_T}$$

- The total energy loss per electron-ion pair lost from the system \mathcal{E}_T is expected to increase with the addition of nitrogen
- So one suggestion was that the secondary electron emission yield explains the observed frequency dependence of the current in the reactive discharge



HiPIMS - Voltage - Current - time

- HiPIMS differs significantly from dcMS, due to the fact that self-sputtering quickly becomes dominant and the working gas ions (mostly Ar⁺ and N₂⁺ or O₂⁺) are depleted from the area in front of the target, due to rarefaction
- The secondary electron emission yield is governed by the composition of the target (Ti or TiN or TiO₂) and the type of ions that are bombarding it



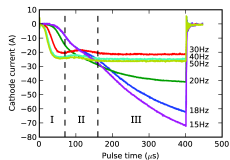
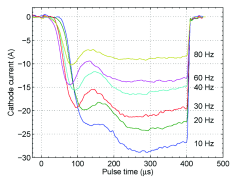
From Magnus et al. (2011), JAP **110** 083306

and Magnus et al. (2012), JVSTA **30** 050601



HiPIMS - Voltage - Current - time

- γ_{SE} is practically zero for singly charged metal ions impacting a target of the same metal
- γ_{SE} will be higher for self sputtering from a TiN or TiO₂ target, where N⁺-ions or O⁺-ions are also present, than for self-sputtering from a Ti target, where multiply charged Ti ions are needed to create secondary electrons



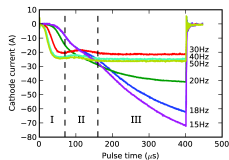
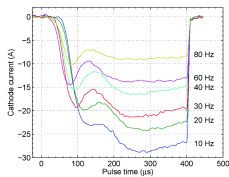
From Magnus et al. (2011), JAP **110** 083306

and Magnus et al. (2012), JVSTA **30** 050601



HiPIMS - Voltage - Current - time

- At high frequencies, nitride or oxide is not able to form between pulses, and self-sputtering by Ti⁺-ions (singly and multiply charged) from a Ti target is the dominant process
- At low frequency, the long off-time results in a nitride or oxide layer being formed on the target surface and self-sputtering by Ti⁺- and N⁺-ions or O⁺-ions from TiN or TiO₂ takes place



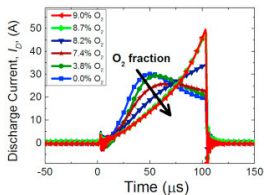
From Magnus et al. (2011), JAP **110** 083306

and Magnus et al. (2012), JVSTA **30** 050601



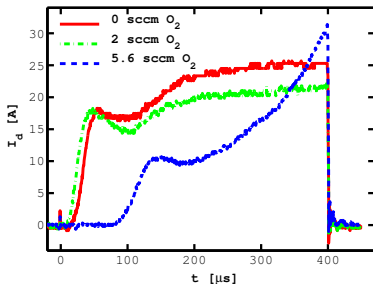
HiPIMS - Voltage - Current - time

- As the oxygen flow is increased a transition to oxide mode is observed



The current waveforms for an Ar/O₂ discharge with a V target where the oxygen flow rate is varied

From Aijaz et al. (2016) Solar Energy Materials and Solar Cells **149** 137



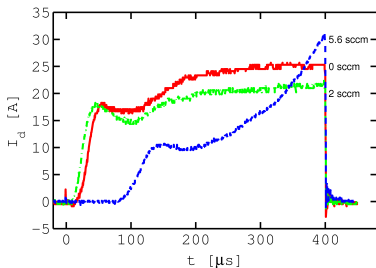
The current waveforms for an Ar/O₂ discharge with a Ti target where the oxygen flow rate is varied – 600 V, 50 Hz and 0.6 Pa

From Gudmundsson et al. (2013), ISSP 2013, p. 192

Gudmundsson (2016) Plasma Phys. Contr. Fus. **58** 014002

HiPIMS - Voltage - Current - time

- The discharge pressure is roughly 0.6 Pa and the pulse voltage is 600 V and this voltage is maintained throughout the pulse.
- The discharge current decreases when 2 sccm of oxygen is added to the discharge
- It has been confirmed that in the oxide mode, the discharge is dominated by O⁺-ions, due to oxygen atoms sputtered off the target surface

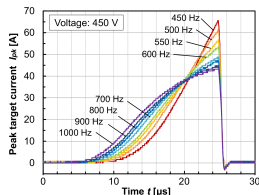
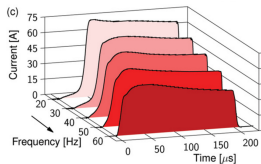


The current waveforms for an Ar/O₂ discharge with a Ti target where the oxygen flow rate is varied – 600 V, 50 Hz and 0.6 Pa

From Gudmundsson et al. (2013), ISSP 2013, p. 192



HiPIMS - Voltage - Current - time



- Similar behaviour has been reported for various target and reactive gas combinations
 - The current increases with decreased repetition frequency
 - The current waveform maintains its shape for Ar/O₂ discharge with Nb target
- The current waveform becomes distinctly triangular for Ar/N₂ discharge with Hf target

From Hála et al. (2012), JPD **45** 055204

From Shimizu et al. (2015), JPD **49** 065202



HiPIMS - Voltage - Current - time

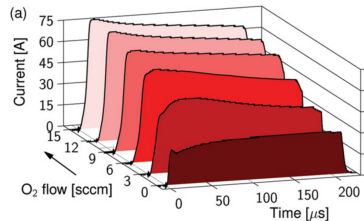
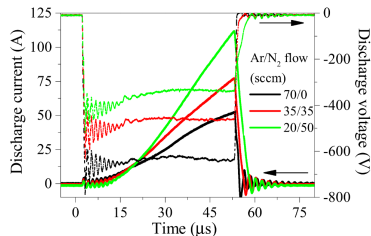
- The current increases with increased partial pressure of the reactive gas

- The current waveform becomes distinctly triangular for Ar/N₂ discharge with Al target

From Moreira et al. (2015), JVSTA **33** 021518

- The current waveform maintains its shape for Ar/O₂ discharge with Nb target

From Hála et al. (2012), JPD **45** 055204



Ionization region model studies of reactive HiPIMS



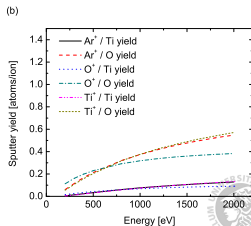
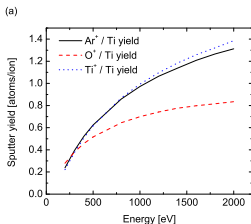
Ionization region model studies of reactive HiPIMS

- The species assumed in the reactive-IRM are
 - cold electrons e^C, hot electrons e^H
 - argon atoms Ar(3s²3p⁶), warm argon atoms in the ground state Ar^W, hot argon atoms in the ground state Ar^H, Ar^m (1s₅ and 1s₃) (11.6 eV), argon ions Ar⁺ (15.76 eV)
 - titanium atoms Ti(a³F), titanium ions Ti⁺ (6.83 eV), doubly ionized titanium ions Ti²⁺ (13.58 eV)
 - oxygen molecule in the ground state O₂(X³Σ_g⁻), the metastable oxygen molecules O₂(a¹Δ_g) (0.98 eV) and O₂(b¹Σ_g) (1.627 eV), the oxygen atom in the ground state O(³P), the metastable oxygen atom O(¹D) (1.96 eV), the positive ions O₂⁺ (12.61 eV) and O⁺ (13.62 eV), and the negative ion O⁻

Ionization region model studies of reactive HiPIMS

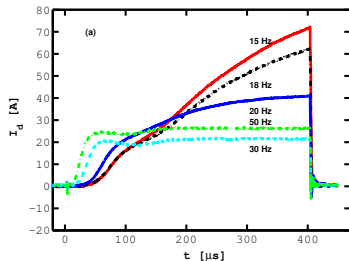
- The sputter yield for the various bombarding ions was calculated by TRIDYN for
 - **Metal mode** – Ti target
 - **Poisoned mode** – TiO₂ target
- The yields correspond to the extreme cases of either clean Ti surface and a surface completely oxidized (TiO₂ surface)
- The sputter yield is much lower for poisoned target

The sputter yield data is from Tomas Kubart, Uppsala University



Ionization region model studies of reactive HiPIMS

- The model is applied to explore Ar/O₂ discharge with Ti target in both metal mode and oxide (poisoned) mode
- The IRM is a semi-empirical model in the sense that it uses a measured discharge voltage and current waveforms as a main input parameter
- For this study we use the measured curve for Ar/O₂ with Ti target at 50 Hz for metal mode and at 15 Hz for poisoned mode

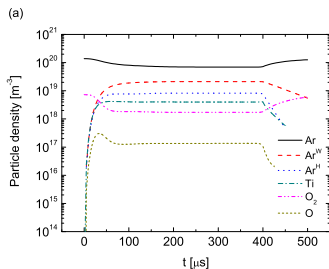


After Magnus et al. (2012), JVSTA **30** 050601



Ionization region model studies of reactive HiPIMS

- The gas rarefaction is observed for the argon atoms but is more significant for the O₂ molecule
- The density of Ti atoms is higher than the O₂ density
- The atomic oxygen density of is over one order of magnitude lower than the molecular oxygen density – the dissociation fraction is low

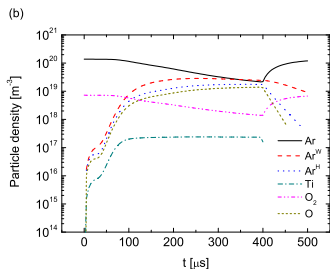


The temporal evolution of the neutral species with 5 % oxygen partial flow rate for Ar/O₂ discharge with Ti target in **metal mode**.

Gudmundsson et al. (2016), PSST, 25(6) 065004

Ionization region model studies of reactive HiPIMS

- Gas rarefaction is observed for both argon atoms and O₂ molecules
- The density of Ti atoms is lower than both the O₂ density and atomic oxygen density
- The atomic oxygen density is higher than the O₂ density towards the end of the pulse



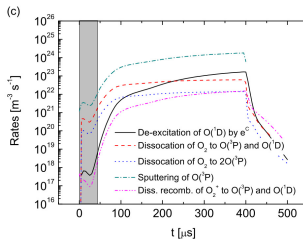
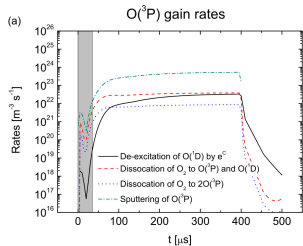
The temporal evolution of the neutral species with **5 % oxygen partial flow** rate for Ar/O₂ discharge with Ti target in **poisoned mode**.

Ionization region model studies of reactive HiPIMS

- The increase in the atomic oxygen in the ground state is due to:
 - sputtering of O(³P) from the partially to fully oxidized target (dominates)
 - electron impact de-excitation of O(¹D)
 - electron impact dissociation of the O₂ ground state molecule

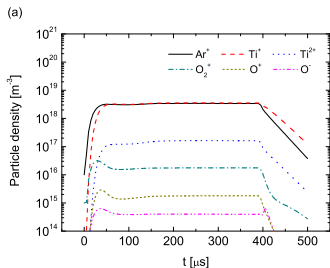
The temporal evolution of the neutral species with 5 % oxygen partial flow rate for Ar/O₂ discharge with Ti target in transition mode and poisoned mode.

Lundin et al. (2017), JAP, 121(17) 171917



Ionization region model studies of reactive HiPIMS

- Ar⁺ and Ti⁺-ions dominate the discharge
- Ti²⁺-ions follow by roughly an order of magnitude lower density
- The O₂⁺ and O⁺-ion density is much lower

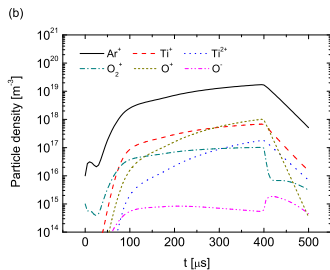


The temporal evolution of the neutral species with **5 % oxygen partial flow** rate for Ar/O₂ discharge with Ti target in **metal mode**.

Gudmundsson et al. (2016), PSST, 25(6) 065004

Ionization region model studies of reactive HiPIMS

- Ar⁺-ions dominate the discharge
- Ti⁺, O⁺, have very similar density, but the temporal variation is different, and the O₂⁺ density is slightly lower
- The Ti²⁺-ion density increases fast with time and overcomes the O₂⁺ density towards the end of the pulse



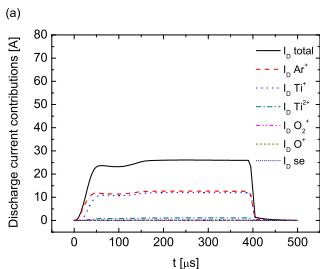
The temporal evolution of the neutral species with **5 % oxygen partial flow** rate for Ar/O₂ discharge with Ti target in **poisoned mode**.

Gudmundsson et al. (2016), PSST, 25(6) 065004



Ionization region model studies of reactive HiPIMS

- Ar⁺ and Ti⁺-ions contribute most significantly to the discharge current at the cathode target surface – almost equal contribution

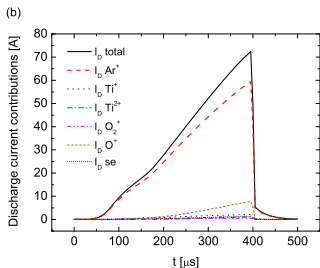


The temporal evolution of the neutral species with **5 % oxygen partial flow rate** for Ar/O₂ discharge with Ti target in **metal mode**.

Gudmundsson et al. (2016), PSST, 25(6) 065004

Ionization region model studies of reactive HiPIMS

- Ar⁺ contribute most significantly to the discharge current – almost solely – at the cathode target surface
- The contribution of secondary electron emission is very small



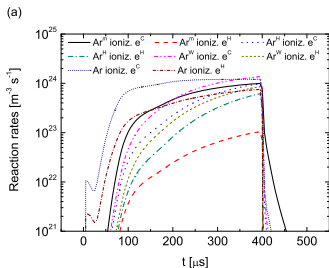
The temporal evolution of the neutral species with **5 % oxygen partial flow rate** for Ar/O₂ discharge with Ti target in **poisoned mode**.

Gudmundsson et al. (2016), PSST, 25(6) 065004



Ionization region model studies of reactive HiPIMS

- Recycling of atoms coming from the target and then ionized are required for the current generation in both modes of operation
- In the metal mode self-sputter recycling dominates and in the poisoned mode working gas recycling dominates
- The dominating type of recycling determines the discharge current waveform



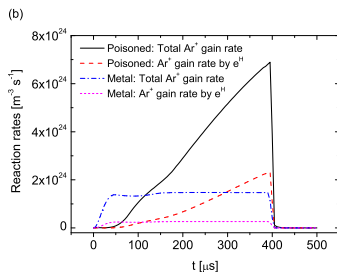
The temporal variations of the reaction rates for electron impact ionization of the argon atoms (ground state plus metastable) in poisoned mode.

Gudmundsson et al. (2016), PSST, 25(6) 065004



Ionization region model studies of reactive HiPIMS

- The temporal variations of the reaction rates for electron impact ionization of the argon atoms (ground state plus metastable)
- The individual rates for all the reactions in the poisoned mode
- The sum of the ionization rates for the e^C plus the e^H populations, and that for the e^H electron population alone



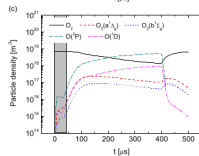
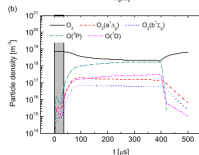
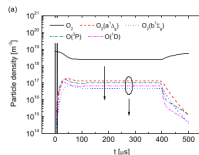
The temporal variations of the reaction rates for the creation of Ar⁺ ions.

Gudmundsson et al. (2016), PSST, **25**(6) 065004

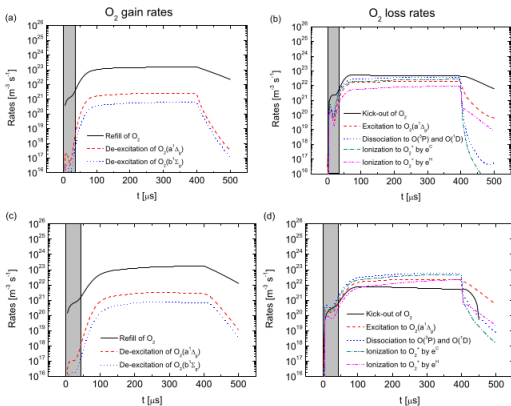


Ionization region model studies of reactive HiPIMS

- The O₂ ground state molecule density which is strongly reduced during the discharge pulse in all modes of operation
- In the metal mode, it is reduced by 67 % during the current plateau at around 300 μs, in the transition mode by 71 % and in the poisoned mode 80 % at the peak discharge current
- At about 200 μs into the pulse in the poisoned mode, the O(³P) becomes more abundant than the O₂ ground state molecule



Ionization region model studies of reactive HiPIMS

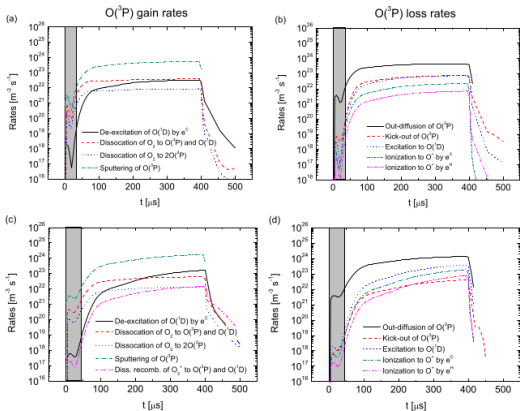


Lundin et al. (2017), JAP **121**(17) 171917

The temporal variations of the most important reaction rates for gain and loss of O₂ ground state molecules in (a-b) transition mode and (c-d) poisoned mode in with **5 % oxygen partial flow rate** for Ar/O₂ discharge with Ti₂ target.



Ionization region model studies of reactive HiPIMS

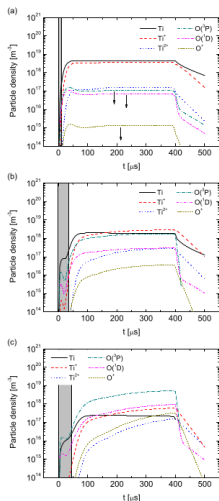
Lundin et al. (2017), JAP **121**(17) 171917

The temporal variations of the most important reaction rates for gain and loss of $\text{O}(\text{3P})$ ground state atom in (a-b) transition mode and (c-d) poisoned mode in with **5 % oxygen partial flow rate** for Ar/O₂ discharge with Ti target.



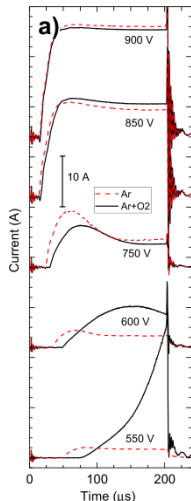
Ionization region model studies of reactive HiPIMS

- The temporal variation of the density of Ti neutrals and ions as well as atomic oxygen neutrals and positive ions
- The Ti ionization fraction increases as we transition from metal mode into poisoned mode
- The ionized flux fraction for Ti towards the end of the pulse is 35 % in metal mode, 49 % in the transition mode, and 64 % in the poisoned mode



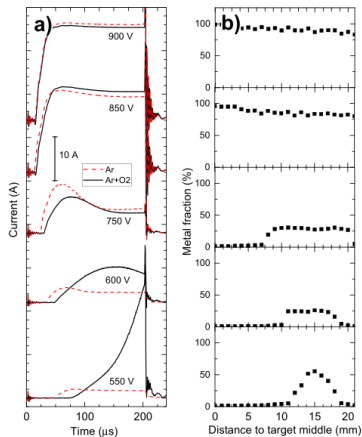
Ionization region model studies of reactive HiPIMS

- The transition to continuously increasing triangular-shaped has been observed experimentally for a Cr target operated in an Ar/O₂ mixture
- Using *in situ* spatially resolved XPS the surface composition of the Cr target was recorded
- Only when the target race track was completely covered by an oxide layer, the triangular pulse shape is observed
- In all other cases, a plateau current was observed



Ionization region model studies of reactive HiPIMS

- If at least 20% of the target area is metallic, then metal atom recycling dominates and a plateau current is observed
- Discharge current waveforms for different applied voltages at discharge frequency of 20 Hz, without and with 0.4% O₂ in the gas mixture
- The profiles of the atomic metal fraction (at%) along the radius of the targets



Ionization region model studies of reactive HiPIMS

- In the metal mode sheath energization was found to be only 10 %
 - same range as the results reported earlier for an Al target
Huo et al. (2013), PSST **22**(4) (2013) 045005
- the dominating electron heating mechanism is Ohmic heating
- For the poisoned mode the sheath energization was 30 %, with a rising trend, at the end of the pulse
 - This is due to the secondary electron emission
 - In the poisoned mode essentially all the ions (mainly Ar⁺, but also O⁺ and Ti²⁺ towards the end of the pulse) contribute to the secondary electron emission
 - In the metal mode only half of the ions contribute to the secondary electron emission (Ar⁺) while the other half does not contribute at all ($\gamma_{\text{Ti}^+} = 0.0$)

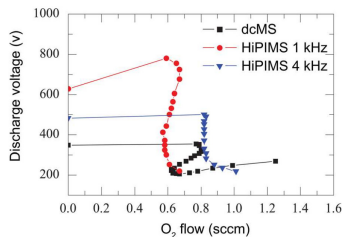


Hysteresis



HiPIMS - Hysteresis

- Typically, a hysteresis effect is seen in reactive sputtering
- The hysteresis effect originates from the changing target conditions due to the reaction of the target surface with the reactive gas
- Sputtering at low reactive gas flows is referred to as metal mode sputtering
- Sputtering at high flows of reactive gas is referred to as compound mode or the poisoned mode sputtering



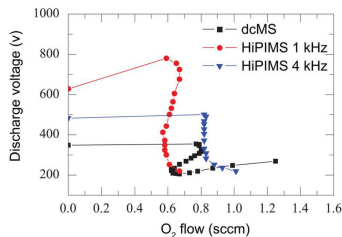
The discharge voltage V_d as a function of the O₂ flow rate during reactive dcMS and HiPIMS of a cerium target.

Aiempanakit et al. (2011), TSP 519 7779



HiPIMS - Hysteresis

- The hysteresis occurs if the effective sputter rate of the compound is lower than for the pure metal
- Also, there is a change in the secondary electron emission yield as compound is formed
- For dcMS – oxygen flow rate in the range 0.6 – 0.8 sccm the discharge can be operated at three different target voltages
 - The upper curve refers to metal mode sputtering
 - The lower curve to compound mode sputtering



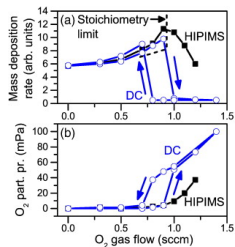
The discharge voltage V_d as a function of the O₂ flow rate during reactive dcMS and HiPIMS of a cerium target.

Aiempanakit et al. (2011), TFS 519 7779



HiPIMS - Hysteresis

- There have been somewhat conflicting reports on the hysteresis effect in HiPIMS discharges
 - Some reports emphasize the need for feedback control (Audronis and Bellido-Gonzalez, 2010; Audronis et al., 2010; Vlček et al., 2013)
 - others report a significant reduction of the hysteresis effect (Sarakinis et al., 2008; Kubart et al., 2011; Aiempanakit et al., 2011)
 - and even elimination (Wallin and Helmersson, 2008; Hála et al., 2012).

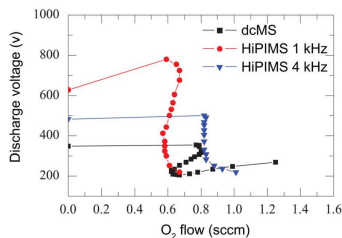


Rate of deposited mass (a) and O₂ partial pressure (b) as a function of O₂ gas flow for HiPIMS and DC sputtering in Ar/O₂ discharge with Al target.

Wallin and Helmersson (2008), TSF 516 6396

HiPIMS - Hysteresis

- Aiempanakit et al. (2011) demonstrate suppression or elimination of the hysteresis
- For a dcMS a relatively wide unstable region is observed while for an HiPIMS the width of the unstable region is substantially smaller
- There is no consensus on the hysteresis effect in the HiPIMS discharge



The discharge voltage V_d as a function of the O₂ flow rate during reactive dcMS and HiPIMS of a cerium target.

Aiempanakit et al. (2011), TSF 519 7779

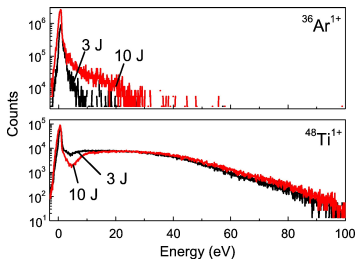


Ion energy and composition



HiPIMS - Ion energy and composition

- For non-reactive HiPIMS the IEDs show
 - the metal ions – an intense high energy tail extending to the limit of the measurement equipment
 - the ions of the working gas exhibit much lower energy
- For comparison the IEDs from dcMS show a peak at an ion energy of about 2 eV and a high-energy tail that extends to around 20 and 40 eV for Ar⁺ and Ti⁺, respectively

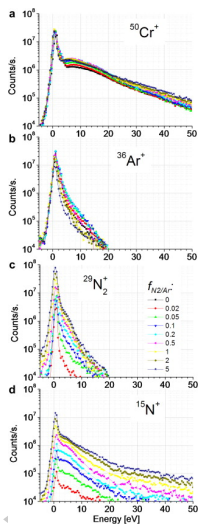


Bohlmark et al. (2006), TSF 515 1522

HiPIMS - Ion energy and composition

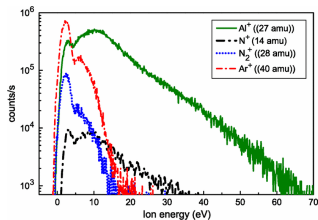
- Reactive Ar/N₂ sputtering of a Cr target
- The Cr⁺ ions comprise an intense low energy peak and pronounced high energy tails
- For reactive sputtering in Ar/N₂ discharges, low energy N₂⁺-ions and energetic N⁺-ions are present in the reactive mode
- The IED for the N⁺-ion possesses a high energy tail just like the Cr⁺-ions (or the Cr²⁺ ions), which is not observed for Ar⁺ or N₂⁺

Greczynski and Hultman (2010), Vacuum **84** 1159



HiPIMS - Ion energy and composition

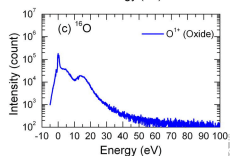
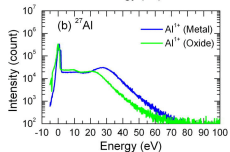
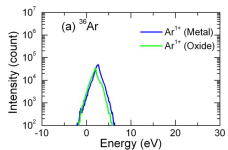
- Similar findings have been reported
 - Ar/N₂ discharge with Ti target – N⁺ behaves like Ti⁺
(Lattemann et al., 2010; Ehiasarian et al., 2007)
 - Ar/N₂ discharge with Al target – N⁺ behaves like Al⁺
(Jouan et al., 2010)
- The working gas ions and the molecular ion of the reactive gas present a similar IED
- The metal ion and the atomic ion of the reactive gas present similar IED and extend to very high energy



Jouan et al. (2010), IEEE TPS **38** 3089

HiPIMS - Ion energy and composition

- The time-averaged ion energy distributions (IED) of the ions in the metal and oxide modes of and Ar/O₂ discharge with Al target
- There is no difference for the distributions of Ar⁺-ions between the metal and oxide modes
- There is a considerable amount of O⁺-ions



Summary



Summary

- The current-voltage-time waveforms in a reactive discharge exhibit similar general characteristics as the non-reactive case in some cases
 - the current rises to a peak, then decays because of rarefaction before rising to a self-sputtering dominated phase
 - in other cases the current develops a triangular shape as repetition frequency is lowered or the partial pressure of the reactive gas is increased
- The secondary electron emission yield is higher for a nitride or oxide target than a titanium target when self-sputtering is the dominant sputtering mechanism



Summary

- An ionization region model was used to explore the plasma composition during the high power pulse
- Comparison was made between the metal mode and the poisoned mode
 - In metal mode Ar⁺ and Ti⁺-ions dominate the discharge and are of the same order of magnitude
 - In poisoned mode Ar⁺-ions dominate the discharge and two orders of magnitude lower, Ti⁺, O⁺, have very similar density, with the O₂⁺ density slightly lower
 - In the metal mode Ar⁺ and Ti⁺-ions contribute most significantly to the discharge current while in poisoned mode Ar⁺ dominate
- In the metal mode self-sputter recycling dominates and in the poisoned mode working gas recycling dominates – the dominating type of recycling determines the discharge current waveform



The slides can be downloaded at

<http://langmuir.raunvis.hi.is/~tumi/ranns.html>

- The work is in collaboration with
 - Dr. Daniel Lundin, Université Paris-Sud, Orsay, France
 - Prof. Nils Brenning, KTH Royal Institute of Technology, Stockholm, Sweden
 - Dr. Michael A. Raadu, KTH Royal Institute of Technology, Stockholm, Sweden
 - Prof. Tiberu Minea, Université Paris-Sud, Orsay, France
- We got help with the sputtering yields from
 - Dr. Tomas Kubart, Uppsala University, Uppsala, Sweden
- and the project has been funded by
 - Icelandic Research Fund Grant No. 130029 and 196141
 - Swedish Government Agency for Innovation Systems (VINNOVA) contract no. 2014-04876,



References

- Agnarsson, B., F. Magnus, T. K. Tryggvason, A. S. Ingason, K. Leosson, S. Olafsson, and J. T. Gudmundsson (2013). Rutile TiO₂ thin films grown by reactive high power impulse magnetron sputtering. *Thin Solid Films* 545, 445–450.
- Aiempanakit, M., A. Aijaz, D. Lundin, U. Helmersson, and T. Kubart (2013). Understanding the discharge current behavior in reactive high power impulse magnetron sputtering of oxides. *Journal of Applied Physics* 113(13), 133302.
- Aiempanakit, M., T. Kubart, P. Larsson, K. Sarakinos, J. Jensen, and U. Helmersson (2011). Hysteresis and process stability in reactive high power impulse magnetron sputtering of metal oxides. *Thin Solid Films* 519(22), 7779–7784.
- Aijaz, A., Y.-X. Ji, J. Montero, G. A. Niklasson, C. G. Granqvist, and T. Kubart (2016). Low-temperature synthesis of thermochromic vanadium dioxide thin films by reactive high power impulse magnetron sputtering. *Solar Energy Materials and Solar Cells* 149, 137–144.
- Anders, A., J. Andersson, and A. Ehasarian (2007). High power impulse magnetron sputtering: Current-voltage-time characteristics indicate the onset of sustained self-sputtering. *Journal of Applied Physics* 102(11), 113303.
- Audronis, M. and V. Bellido-Gonzalez (2010). Hysteresis behaviour of reactive high power impulse magnetron sputtering. *Thin Solid Films* 518(8), 1962 – 1965.
- Audronis, M., V. Bellido-Gonzalez, and B. Daniel (2010). Control of reactive high power impulse magnetron sputtering processes. *Surface and Coatings Technology* 204(14), 2159–2164.
- Bohlmark, J., M. Lattemann, J. T. Gudmundsson, A. P. Ehasarian, Y. A. Gonzalvo, N. Brenning, and U. Helmersson (2006). The ion energy distributions and ion flux composition from a high power impulse magnetron sputtering discharge. *Thin Solid Films* 515(5), 1522–1526.
- Bradley, J. W., A. Mishra, and P. J. Kelly (2015). The effect of changing the magnetic field strength on HiPIMS deposition rates. *Journal of Physics D: Applied Physics* 48(21), 215202.
- Ehasarian, A. P., Y. A. Gonzalvo, and T. D. Whitmore (2007). Time-resolved ionisation studies of the high power impulse magnetron discharge in mixed argon and nitrogen atmosphere. *Plasma Processes and Polymers* 4(S1), S309–S313.



References

- Greczynski, G. and L. Hultman (2010). Time and energy resolved ion mass spectroscopy studies of the ion flux during high power pulsed magnetron sputtering of Cr in Ar and Ar/N₂ atmospheres. *Vacuum* 84(9), 1159 – 1170.
- Gudmundsson, J. T. (2008). Ionized physical vapor deposition (IPVD): Magnetron sputtering discharges. *Journal of Physics: Conference Series* 100, 082002.
- Gudmundsson, J. T. (2016). On reactive high power impulse magnetron sputtering. *Plasma Physics and Controlled Fusion* 58(1), 014002.
- Gudmundsson, J. T., N. Brenning, D. Lundin, and U. Helmersson (2012). The high power impulse magnetron sputtering discharge. *Journal of Vacuum Science and Technology A* 30(3), 030801.
- Gudmundsson, J. T., D. Lundin, N. Brenning, M. A. Raadu, C. Huo, and T. M. Minea (2016). An ionization region model of the reactive Ar/O₂ high power impulse magnetron sputtering discharge. *Plasma Sources Science and Technology* 25(6), 065004.
- Gudmundsson, J. T., F. Magnus, T. K. Tryggvason, S. Shayestehaminzadeh, O. B. Sveinsson, and S. Olafsson (2013). Reactive high power impulse magnetron sputtering. In *Proceedings of the XII International Symposium on Sputtering and Plasma Processes (ISSP 2013)*, pp. 192–194.
- Hajihoseini, H. and J. T. Gudmundsson (2017). Vanadium and vanadium nitride thin films grown by high power impulse magnetron sputtering. *Journal of Physics D: Applied Physics* 50(50), 505302.
- Hála, M., J. Čapek, O. Zabeida, J. E. Klemberg-Sapieha, and L. Martinu (2012). Hysteresis - free deposition of niobium oxide films by HiPIMS using different pulse management strategies. *Journal of Physics D: Applied Physics* 45(5), 055204.
- Helmersson, U., M. Lattemann, J. Bohlmark, A. P. Ehasarian, and J. T. Gudmundsson (2006). Ionized physical vapor deposition (IPVD): A review of technology and applications. *Thin Solid Films* 513(1-2), 1–24.
- Huo, C., D. Lundin, J. T. Gudmundsson, M. A. Raadu, J. W. Bradley, and N. Brenning (2017). Particle-balance models for pulsed sputtering magnetrons. *Journal of Physics D: Applied Physics* 50(35), 354003.
- Huo, C., D. Lundin, M. A. Raadu, A. Anders, J. T. Gudmundsson, and N. Brenning (2013). On sheath energization and ohmic heating in sputtering magnetrons. *Plasma Sources Science and Technology* 22(4), 045005.
- Huo, C., M. A. Raadu, D. Lundin, J. T. Gudmundsson, A. Anders, and N. Brenning (2012). Gas rarefaction and the time evolution of long high-power impulse magnetron sputtering pulses. *Plasma Sources Science and Technology* 21(4), 045004.

References

- Jouan, P.-Y., L. Le Brizoual, C. Cardinaud, S. Tricot, and M. A. Djouadi (2010). HiPIMS ion energy distribution measurements in reactive mode. *IEEE Transactions on Plasma Science* 38(11), 3089–3094.
- Kubart, T., M. Aiempanakit, J. Andersson, T. Nyberg, S. Berg, and U. Helmersson (2011). Studies of hysteresis effect in reactive HiPIMS deposition of oxides. *Surface and Coatings Technology* 205(Supplement 2), S303–S306.
- Lattemann, M., U. Helmersson, and J. E. Greene (2010). Fully dense, non-faceted 111-textured high power impulse magnetron sputtering TiN films grown in the absence of substrate heating and bias. *Thin Solid Films* 518(21), 5978–5980.
- Layes, V., C. C. Roca, S. Monje, V. Schulz-von der Gathen, A. von Keudell, and T. de los Arcos (2018). Connection between target poisoning and current waveforms in reactive high power impulse magnetron sputtering of chromium. *Plasma Sources Science and Technology* 27(8), 084004.
- Leosson, K., S. Shayestehaminzadeh, T. K. Tryggvason, A. Kossov, B. Agnarsson, F. Magnus, S. Olafsson, J. T. Gudmundsson, E. B. Magnusson, and I. A. Shelykh (2012). Comparing resonant photon tunneling via cavity modes and Tamm plasmon polariton modes in metal-coated Bragg mirrors. *Optics Letters* 37(19), 4026–4028.
- Lundin, D., J. T. Gudmundsson, N. Brenning, M. A. Raadu, and T. M. Minea (2017). A study of the oxygen dynamics in a reactive Ar/O₂ high power impulse magnetron sputtering discharge using an ionization region model. *Journal of Applied Physics* 121(17), 171917.
- Magnus, F., A. S. Ingason, S. Olafsson, and J. T. Gudmundsson (2012). Nucleation and resistivity of ultrathin TiN films grown by high power impulse magnetron sputtering. *IEEE Electron Device Letters* 33(7), 1045 – 1047.
- Magnus, F., O. B. Sveinsson, S. Olafsson, and J. T. Gudmundsson (2011). Current-voltage-time characteristics of the reactive Ar/N₂ high power impulse magnetron sputtering discharge. *Journal of Applied Physics* 110(8), 083306.
- Magnus, F., T. K. Tryggvason, S. Olafsson, and J. T. Gudmundsson (2012). Current-voltage-time characteristics of the reactive Ar/O₂ high power impulse magnetron sputtering discharge. *Journal of Vacuum Science and Technology A* 30(5), 050601.



References

- Moreira, M. A., T. Törndahl, I. Katardjiev, and T. Kubart (2015). Deposition of highly textured AlN thin films by reactive high power impulse magnetron sputtering. *Journal of Vacuum Science and Technology A* 33(2), 021518.
- Raadu, M. A., I. Axnäs, J. T. Gudmundsson, C. Huo, and N. Brenning (2011). An ionization region model for high power impulse magnetron sputtering discharges. *Plasma Sources Science and Technology* 20(6), 065007.
- Sarakinos, K., J. Alami, C. Klever, and M. Wuttig (2008). Process stabilization and enhancement of deposition rate during reactive high power pulsed magnetron sputtering of zirconium oxide. *Surface and Coatings Technology* 202(20), 5033 – 5035.
- Shimizu, T., M. Villamayor, D. Lundin, and U. Helmersson (2015). Process stabilization by peak current regulation in reactive high-power impulse magnetron sputtering of hafnium nitride. *Journal of Physics D: Applied Physics* 49(6), 065202.
- Toneli, D. A., R. S. Pessoa, M. Roberto, and J. T. Gudmundsson (2015). On the formation and annihilation of the singlet molecular metastables in an oxygen discharge. *Journal of Physics D: Applied Physics* 48(32), 325202.
- Vlček, J., J. Rezek, J. Houška, R. Čerstvý, and R. Bugyi (2013). Process stabilization and a significant enhancement of the deposition rate in reactive high-power impulse magnetron sputtering of ZrO₂ and Ta₂O₅ films. *Surface and Coatings Technology* 236, 550–556.
- Wallin, E. and U. Helmersson (2008). Hysteresis-free reactive high power impulse magnetron sputtering. *Thin Solid Films* 516(18), 6398 – 6401.

